Supporting Information

Azine-Linked Covalent Organic Framework ACOF-1 Membrane for Highly Selective CO_2/CH_4 Separation

Hongwei Fan,*[a,b] Alexander Mundstock,[a] Jiahui Gu,[b] Hong Meng[b] and Jürgen Caro*[a]

[a]*Institute of Physical Chemistry and Electrochemistry, Leibniz Universität Hannover, Callinstraße 3A, D-30167 Hannover, Germany.*

[b]*College of Chemical Engineering, Beijing University of Chemical Technology, Beijing 100029, PR China.*

E-mail: hongwei.fan@pci.uni-hannover.de; juergen.caro@pci.uni-hannover.de

1. Experimental Section

Materials: All chemicals were used as received: hydrazine hydrate (99%, Aldrich), 1,3,5-triformylbenzene (TFB) (96%, Ark), acetic acid 36% (AR, Roth), 1,4-dioxane (>99%, Acros), ethanol (>99%, Acros), polyethyleneimine (PEI) (50 wt% in water, Aldrich). Porous Al_2O_3 disks (Fraunhofer IKTS, former Hermsdorfer HITK, Germany) as supports are 18 mm in diameter and 1 mm in thickness. The pore size is 70 nm on the top layer of the disk.

PEI modification of the support surface: Porous Al_2O_3 support was immersed in HCl solution (1 M in 25 mL of pure water) at room temperature for 6 h to activate the surface hydroxyl groups, then being water-washed until neutral and dried. The as-activated Al_2O_3 support was immersed in PEI aqueous solution (50 mg PEI in 10 mL water) for 20s and subsequently dried. This procedure was repeated several times to ensure the deposition of an unifrom amino layer deposited on the support surface.

Synthesis of azine-linked covalent organic framework ACOF-1 membrane: Firstly, the PEI-modified Al_2O_3 support surface was grafted with aldehyde groups by reaction with TFB (20 mg in 5 mL dioxane) at 150 ℃ for 1 h. After washed and dried, the aldehyde-Al_2O_3 support was placed horizontally face up in a Teflon-lined stainless steel autoclave which was filled with synthesis solution (100 mg TFB, 63.3 μL hydrazine hydrates in 5 mL dioxane in the presence of 0.5 mL 6M acetic acid), and then heated at 120 ℃ for 72 h. A continuous and defect-free ACOF-1 membrane was obtained after washing with dioxane, ethanol, and drying at 120 ℃ overnight.

Characterization of ACOF-1 membrane and powder: Micro-morphologies of membranes and powders samples were performed on a JEOL JSM-6700F instrument with a cold field emission gun operating at 2 kV and 10 mA. Before measurement, all samples were coated with a 15-nm thick gold layer in vacuum to reduce charging effects. Elemental analysis of the membrane cross-section was performed on the JSM-6700F instrument at 15 kV, 10 mA and 15 mm lense distance. The X-ray diffraction (XRD) patterns were recorded on a Bruker D8 Advance diffractometer (Cu K_α X-ray radiation, $\lambda = 1.54$ Å) at room temperature, and each XRD pattern was acquired from 3 ° to 35 ° at a rate of $0.01\ °s^{-1}$ (at a voltage of 40 kV and current of 40 mA).

Gas separation measurement: The prepared ACOF-1 membrane was fixed in a Wicke–Kallenbach permeation apparatus (Figure S5) sealed with O-rings. A 1:1 mixture of CO_2/CH_4 was applied to the feed side of the membrane, and the feed flow rate was kept constant at 100 mL min^{-1} (each gas of 50 mL min^{-1}). N_2 was used as the sweep gas, and the pressures at both sides were kept at 1 bar. A calibrated gas chromatograph (HP 6890B) was used to measure the concentration of mixed gases on the permeate side after the system reached the stable state. The single gas permeation measurement is similar to that of the mixture gas. The feed flow rates and the pressures at both sides were set to 50 ml min^{-1} and 1 bar. In most of the cases, N_2 was used as sweep gas, except in the N_2 measurement, where CH_4 was employed as the sweep gas. At least three parallel membranes were measured in exactly the same manner. Each membrane was analyzed at least 10 times by using the same evaluation conditions. The error bar represents the standard deviation of the average permeance obtained from independent measurements. The error estimates represent the relative standard deviation calculated by dividing the standard deviation by the mean and multiplied by 100. The separation factor $\alpha_{i,j}$ of a binary mixture is defined as the quotient of the molar ratios of the components (*i,j*) in the permeate, divided by the quotient of the molar ratio of the components (*i,j*) in the feed:

$$\alpha_{i,j} = \frac{X_{i,p} / X_{j,p}}{X_{i,f} / X_{j,f}} .$$

2. Figures and Tables

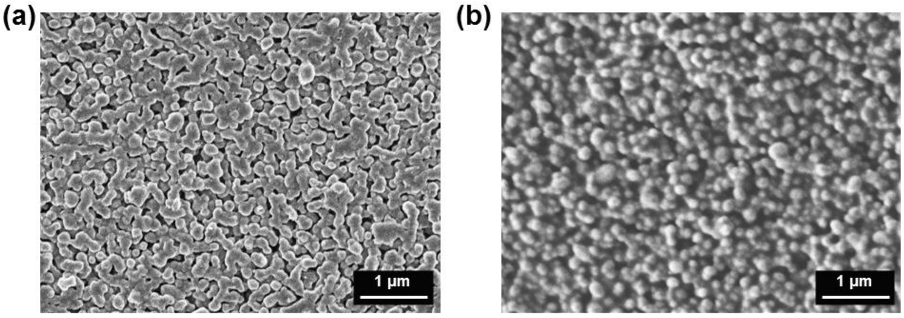

Fig. S1 Surface SEM images of (a) original α-Al_2O_3 support, (b) PEI-modified α-Al_2O_3 support.

As compared to the original porous α-Al_2O_3 support (Fig. S1a), the modified surface (Fig. S1b) becomes blurry indicating a uniform PEI layer coated on it.

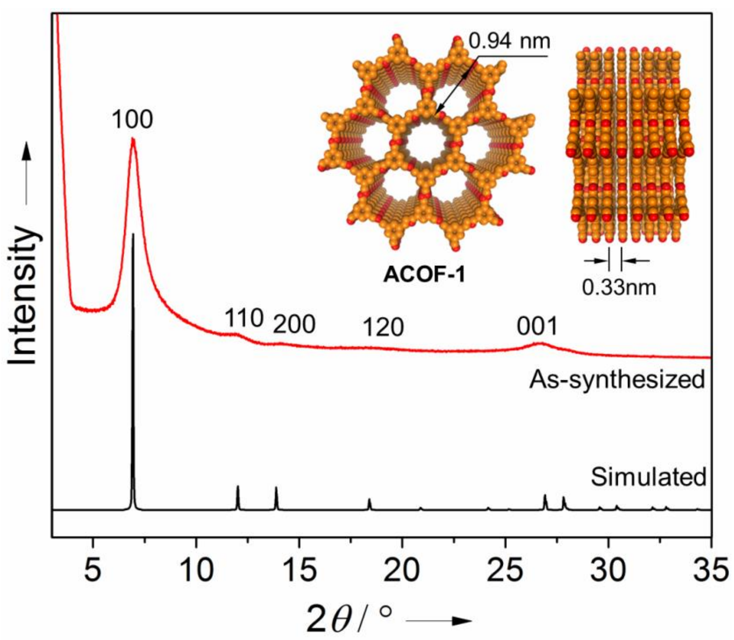

Fig. S2 Simulated (black line) and experimental (red line) PXRD patterns of ACOF-1 in 2D eclipsed stacking (inset images show crystal structures viewed through [001] (left) and [100] (right) directions). The simulated patterns were made by materials studio 8.0.

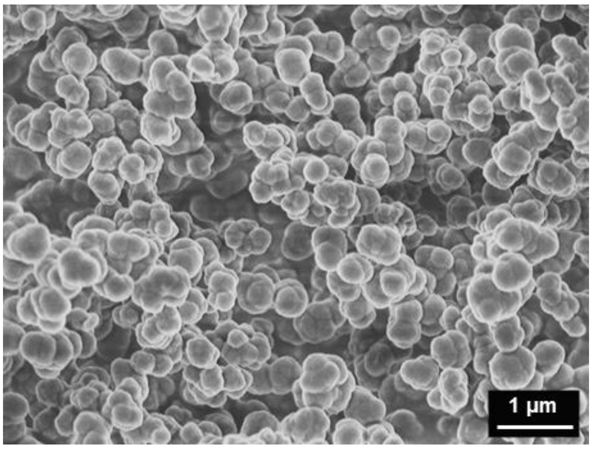

Fig. S3 SEM image of the ACOF-1 powders collected from the Teflon-lined stainless steel autoclave after synthesis of membrane. The particle size is about 400-500 nm in diameter.

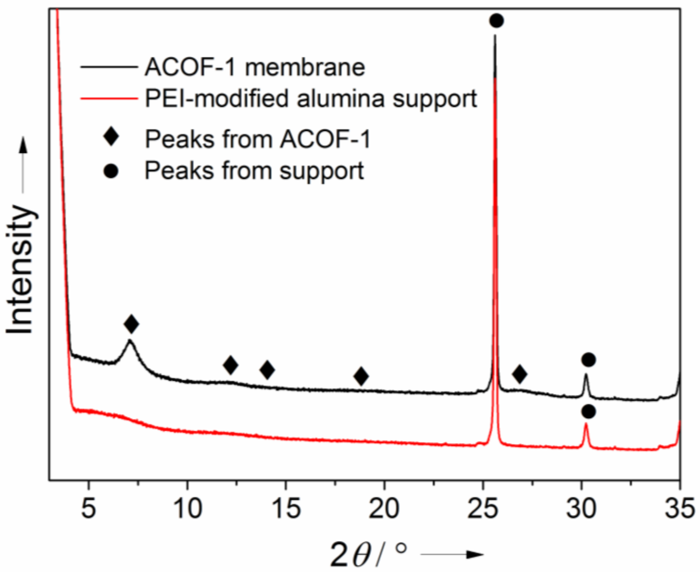

Fig. S4 XRD patterns of the synthesized ACOF-1 membrane on PEI-modified alumina supports.

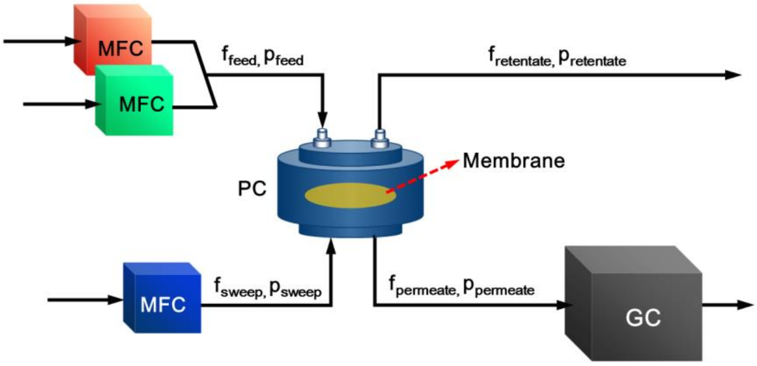

Fig. S5 Measurement equipment for mixed gas permeations. MFC: mass flow controller; PC: permeation cell with mounted membrane; GC: gas chromatograph; f: volumetric flow rate; p: pressure.

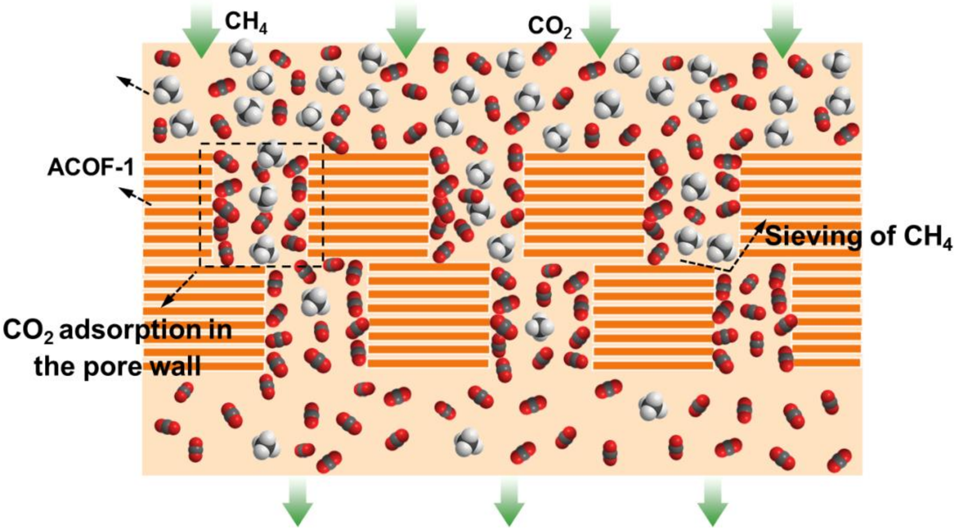

Fig. S6 Schematic diagram of possible separation mechanism for the CO_2/CH_4 gas pair in ACOF-1 membrane.

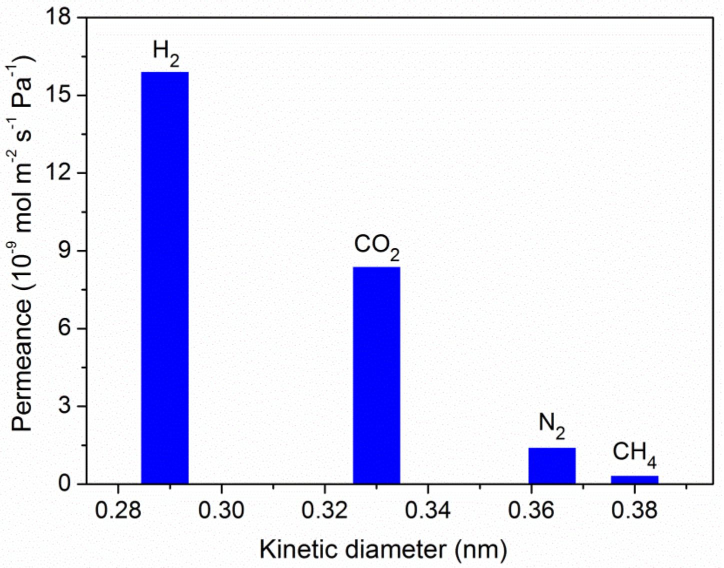

Fig. S7 Single gas permeances of the ACOF-1 membrane measured at 120 ℃ and 1 bar.

As shown in Fig. S7, the smaller gas molecules of H_2 and CO_2 show larger permeance than the bulky molecules of N_2 and CH_4, and there is a cutoff observed between them. It is noteworthy that the single gas CH_4 permeance (3.14×10^{-10} mol m^{-1} s^{-1} Pa^{-1}) is nearly 3 times larger than the CH_4 permeance in the CO_2/CH_4 mixture (1.1×10^{-10} mol m^{-1} s^{-1} Pa^{-1}). This finding indicates that the strong adsorption of CO_2 inside the ACOF-1 pores reduces the CH_4 mobility in addition to the confinement effect. The single gas CO_2 permeance is almost unchanged in comparison with the mixture and even slightly lower than that of the CO_2/CH_4 mixtures. This is due to the excessive adsorption of CO_2 in the pores blocking the diffusive channels for CH_4.

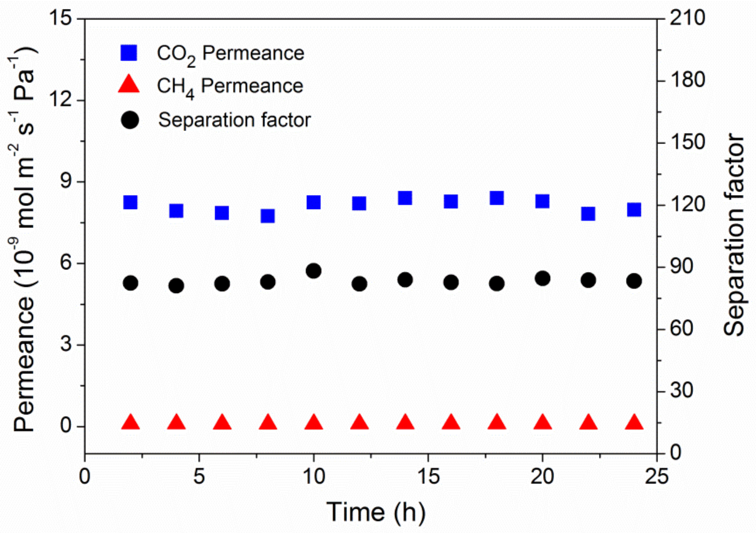

Fig. S8 Performance measurement of the ACOF-1 membrane for the separation of an equimolar CO_2/CH_4 mixture with adding of 3 mol% steam at 120 ℃ and 1 bar.

The hydrothermal stability of the ACOF-1 membrane was tested by separating an equimolar CO_2/CH_4 mixture containing 3 mol % steam at 120 ℃ and 1 bar for 24 h. The CO_2/CH_4 mixed gas with total flow rate of 100 ml min^{-1} and pressure of 1 bar bubbled through a water saturator at room temperature (25 ℃) before entering the permeation cell.[S1] The steam concentration in this feed is around 3 mol%. As shown in Fig. S8, the ACOF-1 membrane also exhibits a high stability in the presence of steam, and both CO_2 permeance and CO_2/CH_4 selectivity are fluctuated slightly during the measurement, which shows that the ACOF-1 pore volume is not blocked by adsorbed water. The slight reduction of the CO_2 permeance is due to the parallel permeation of H_2O and CO_2 through the ACOF-1 membrane, considering the small kinetic diameter of H_2O (0.26 nm).

Table S1 A summary of the CO_2/CH_4 separation performance of membranes in this work and in reported literatures.

Membrane	Thickness (μm)	Temperature (℃)	Pressure (Bar)	CO_2 permeability* (Barrer)	SF (CO_2/CH_4)	Ref.
6FDA-Bisp	30–60	35	2	108	41.9	[S2]
NH_2-MIL-53(Al)/CA	--	25	3	52.6	$28.7^{\dagger}$	[S3]
Pebax–PCNs-10	50-80	25	2	520	51	[S4]
S-10	65	75	5	205.1	12	[S5]
PIM-co-UiO-$66_{72\ h}$	--	25	2	12498	$31.9^{\dagger}$	[S6]
BTDA-CADA1-450	80	35	1	$1022^{\#}$	$26.5^{\#}$	[S7]
F-SPEEK/4A	4	25	5	49.2	55	[S8]
Fe-PVDF	< 100	35	--	5.3	5.6	[S9]
TB–CMS-800	100–120	35	1	1406	112	[S10]
ZIF-7-8	1-2	25	1	350	4.3	[S11]
Ultrathin-MMMs	0.66	30	1	268.62	15.6	[S12]
TSI-100	20-60	35	8	9.6	25	[S13]
RTIL-modified SSZ-13	10	RT	2	2987.7	87	[S14]
Z32-IP	< 10	30	2	288	16	[S15]
PIL-IL 75	148	25	1	525	18	[S16]
MIL-53-NH_2/organosilica	0.1	25	2	430	18.2	[S17]
P84/cPIM-1	40	35	3.5	2061.0	20.4	[S18]
HKUST-1 MMM	50-70	25	2	$1101.6^{\#}$	$29.3^{\#}$	[S19]
Matrimid/Sm-NaY	45-55	35	2	$9.70^{\#}$	$57.1^{\#}$	[S20]
$Zn(pyrz)_2(SiF_6)$/XLPEO	--	25	1	590	30	[S21]
NH_2-MIL-125(Ti)/PSF	10	30	3	40	29.2	[S22]
TPDA–APAF	40-60	35	20	30	50	[S23]
ZIF-69	40	25	3	2820.4	4.6	[S24]
NUS-2@Ultem	50−100	35	2	$8.7^{\#}$	$12.7^{\#}$	[S25]
NUS-3@Ultem	50−100	35	2	$8.1^{\#}$	$10.7^{\#}$	[S25]
ACOF-1/Matrimid	47	30	4	15.3	32.4	[S26]
TpPa-1(50)@PBI-BuI	70.24	RT	20	13.1	40.3	[S27]
TpBD(50)@PBI-BuI	82.44	RT	20	14.8	48.7	[S27]
ACOF-1	8	25	1	56.64	97.1	This work
ACOF-1	8	120	1	237.1	86.4	This work
ACOF-1	8	120	2	216.4	60.1	This work

$^{\#}$ Ideal separation factor.

CO_2 permeability in Barrer is calculated as the membrane permeance multiplied by the membrane thickness. 1 Barrer = 3.347×10^{-16} mol m^{-1} s^{-1} Pa^{-1}

3. References

[S1] Y. Li, F. Liang, H. Bux, W. Yang and J. Caro, *J. Membr. Sci*., 2010, **354**, 48.

[S2] M. Z. Ahmad, M. Navarro, M. Lhotka, B. Zornoza, C. Téllez, V. Fila and J. Coronas, *Sep. Purif. Technol.*, 2018, **192**, 465–474.

[S3] M. Mubashir, Y. Y. Fong, L. K. Keong, C. T. Leng and N. Jusoh.Voigt, *Sep. Purif. Technol.*, 2018, **199**, 140–151.

[S4] J. Hou, X. Li, R. Guo, J. Zhang and Z. Wang, *Nanotechnology*, 2018, **29**, 125706.

[S5] M. Isanejad and T. Mohammadi. *Mater, Chem. Phy*s., 2018, **205**, 140–151.

[S6] N. Tien-Binh, D. Rodrigue and S. Kaliaguine, *J. Membr. Sci*., 2018, **548**, 429–438.

[S7] C. Zhang, P, Li and B. Cao, *J. Membr. Sci*., 2018, **528**, 206–216.

[S8] Z. Tahir, A. Ilyas, X. Li, M. R. Bilad, I. F. J. Vankelecom and A. L. Khan, *J. Appl. Polym. Sci*., 2018, **135**, 45952.

[S9] S. Das and T. Ben, *Dalton Trans*., 2018, **47**, 7206.

[S10] Z. Wang, H. Ren, S. Zhang, F. Zhang and J. Jin, *ChemSusChem*, 2018, **11**, 1–9

[S11] F. Hillman, J. Brito and H. K. Jeong, *ACS appl. Mater. Inter.*, 2018, **10**, 5586–5593.

[S12] Y. Cheng, X. Wang, C. Jia, Y. Wang, L. Zhai, Q. Wang and D. Zhao, *J. Membr. Sci*., 2017, **539**, 213–223.

[S13] V. Martin-Gil, A. López, P. Hrabanek, R. Mallada, I. F. J. Vankelecom and V. Fila, *J. Membr. Sci*., 2017, **523**, 24–35.

[S14] B. Liu, R. Zhou, N. Bu, Q. Wang, S. Zhong, B. Wang and K. Hidetoshi, *J. Membr. Sci*., 2017, **524**, 12–19.

[S15] A. Jomekian, B. Bazooyar, R. M. Behbahani, T. Mohammadi and A. Kargari, *J. Membr. Sci*., 2017, **524**, 652–662.

[S16] K. Friess, M. Lanč, K. Pilnáček, V. Fíla, O. Vopička, Z. Sedláková, M. G. Cowan, W. M. McDanel, R. D. Noble, D. L. Gind and P. Izak, *J. Membr. Sci*., 2017, **528**, 64–71.

[S17] C. Kong, H. Du, L. Chen and B. Chen, *Energy Environ. Sci.*, 2017, **10**, 1812–1819.

[S18] P. Salehian, W. F. Yong and T. S. Chung, *J. Membr. Sci*., 2016, **518**, 110–119.

[S19] R. Lin, L. Ge, H. Diao, V. Rudolph and Z. Zhu, *ACS Appl. Mater. Interfaces.*, 2016, **8**, 32041−32049.

[S20] A. E. Amooghin, M. Omidkhah and A. Kargari, *J. Membr. Sci*., 2015, **490**, 364–379.

[S21] H. Gong, T. H. Nguyen, R. Wang and T. H. Bae, *J. Membr. Sci*., 2015, **495**, 169–175.

[S22] X. Guo, H. Huang, Y. Ban, Q. Yang, Y. Xiao, Y. Li, W. Yang and C. Zhong, *J. Membr. Sci.*, 2015, **478**, 130–139.

[S23] R. Swaidan, B. Ghanem, E. Litwiller and I. Pinnau, *J. Membr. Sci*., 2015, **475**, 571–581.

[S24] Y. Liu, G. Zeng, Y. Pan and Z. Lai, *J. Membr. Sci*., 2011, **379**, 46.

[S25] Z. Kang, Y. Peng, Y. Qian, D. Yuan, M. A. Addicoat, T. Heine, Z. Hu, L. Tee, Z. Guo and D. Zhao, *Chem. Mater.*, 2016, **28**, 1277–1285.

[S26] M. Shan, B. Seoane, E. Rozhko, A. Dikhtiarenko, G. Clet, F. Kapteijn and J. Gascon, *Chem. Eur. J*., 2016, **22**, 14467–14470.

[S27] B. P. Biswal, H. D. Chaudhari, R. Banerjee and U. K. Kharul, *Chem. Eur. J*., 2016, **22**, 4695–4699.